Int. J. Electrochem. Sci., 4 **(2009)** 1735 - 1753

International Journal of ELECTROCHEMICAL SCIENCE
www.electrochemsci.org

Effect of a poly(ethylene glycol) (MW 200)/benzylideneacetone Additive Mixture on Zn Electrodeposition in an Acid Chloride Bath

L.E. Morón. Y. Meas, R. Ortega-Borges, J.J. Perez-Bueno, H. Ruiz, G. Trejo[*]

Centro de Investigación y Desarrollo Tecnológico en Electroquímica (CIDETEQ). Parque Tecnológico Sanfandila, Pedro Escobedo, Querétaro, A. P. 064. C.P. 76703, Querétaro, México
[*]E-mail: gtrejo@cideteq.mx

Received: 14 October 2009 / *Accepted:* 1 December 2009 / *Published:* 31 December 2009

The influence of two additives—poly(ethylene glycol) (MW 200) (PEG_{200}) alone and a mixture of PEG_{200} and benzylideneacetone (PEG_{200}/BDA)—on the mechanism of Zn electroreduction and the morphological characteristics of the coatings obtained was studied. A study of the adsorption of additive molecules onto a Fe electrode surface at the open circuit potential (E_{OCP}) using a quartz crystal microbalance (QCM) disclosed that both PEG_{200} and PEG_{200}/BDA were adsorbed on the electrode, with a higher mass increase being observed for the system with PEG_{200}/BDA. Cyclic voltammetry showed that the adsorption of PEG_{200}/BDA partially inhibited the electroreduction of Zn at E = -1.12 V vs. SCE. This inhibition caused an increase in the overpotential for the discharge of Zn(II) ions, resulting in two reduction processes with different energies. A study of the reduction kinetics revealed that for both the PEG_{200} and PEG_{200}/BDA systems, the adsorption of additive molecules onto the electrode surface caused a decrease in the exchange current density (i_0), which made the kinetics of the process slower. When PEG_{200} or PEG_{200}/BDA was present in the electrolytic bath, the values of α_c were slightly lower; this effect is associated with differences in the morphologies of coatings grown in the presence of additive molecules. The coatings grown in the presence of the PEG_{200}/BDA additive mixture were compact, smooth and shiny materials comprised of flakes grouped in hemispherical clusters of uniform size.

Keywords: Additives, Benzylideneacetone, Electrodeposition, Poly(ethylene glycol), Zinc

1. INTRODUCTION

Zinc electrodeposits are of practical and industrial importance due to their proven ability to protect ferrous substrates against corrosion [1-5]. In efforts to achieve better corrosion protection, both alkaline [6,7] and acid electrochemical processes have been developed. Each of these approaches has

advantages and disadvantages. In general, acid baths exhibit higher cathode current efficiencies but are characterized by poor deposit distribution on the substrate. The higher cathode current efficiencies of such baths afford the added advantage of allowing plating over hardened steel and cast iron. Alkaline processes tend to have lower cathode current efficiencies but exhibit very good plate distribution and contain complexes that effect waste treatment. In particular, the acidic process for the electrodeposition of Zn can use sulfate [8,9,10,11] or chloride electrolytic baths [12,13,14,15,16].

Diverse factors influence the mechanism of Zn electrodeposition, including the morphology of the coating that is formed. Recent work by Raeissi et al. [17] showed that temperature, pH, and current density affect the morphology, texture, and nucleation mechanism of Zn deposits. Yu et al. observed that increasing the temperature increased the nucleation density and modified the nucleation mechanism of Zn electrodeposits [18]. In addition, it has been shown that the concentration of Zn(II) ions [19], complexing agents [20], anions [21,22] and organic additives [23] play fundamental roles in Zn electrodeposition. The use of additives in electrolytic baths is very important due to their influence on the growth and structure of the deposits obtained. In particular, organic additives block part of the electrode surface, thereby reducing the number of active sites for nucleus formation and hence decreasing the nucleation rate. The adsorption of an additive can decrease the rate of nucleation for two reasons. First, additive molecules may block the electrode surface and reduce the frequency of appearance of sub-critical clusters. Second, they may block the surface of the critical nuclei and impede the incorporation of single ions [16]. Typically, additives are added to the electrolytic bath at concentrations on the order of parts per million; their presence in the bath promotes the formation of soft and shiny coatings. In addition, additives can cause modifications of other physical characteristics of the coatings; for example, Mirkova et al. [24] found that hydrogenation of a steel substrate was strongly reduced in the presence of an additive mixture composed of PEG_{6000}, Na–benzoate, ethanol and benzalacetone and Song et al. [25] showed that addition of poly(ethylene glycol) (PEG) and gelatin to the electrolytic bath inhibits hydrogen adsorption on the deposited Zn. In recent years, benzoic acid (BA), BDA [26-28] and PEG [29-32] have been increasingly used as additives in the electrodeposition of Zn and Zn-Co alloys [33] in acid baths. The superior quality of the coatings obtained in the presence of these additives has generated growing interest in the effects of these compounds on the morphology and physical properties of the coatings. Recent studies by Su-Moon et al. [34,35] have shown that BA controls the roughness of Zn coatings, an effect that was attributed to the adsorption of BA onto active sites on the substrate. -Danciu et al. [36] reported similar results when BDA was used as a primary brightener in the electrodeposition of Zn coatings. They showed that addition of a range of brighteners, including BDA, caused a significant displacement of the potentiodynamic curves toward more negative potentials. In other work in this area, Juhos et al. [37] showed that addition of BDA increases the capacitance of the double layer, and Bernotiene and Mockute. [27,38] found that addition of BA into a bath containing BDA caused a decrease in the rate of BDA consumption. However, PEG molecules raise the overpotentials for reduction of both Zn(II) ions and protons by effectively blocking the electrode surface. In studies on the electrodeposition of Zn in the presence of PEG, Kim et al. [39] found that PEG molecules adsorbed on an iron surface form ordered structures and appear to desorb in the underpotential deposition region of Zn(II) ions. In

addition, using the quartz crystal microbalance (QCM) technique, Mendez et al. [40] showed that PEG_{20000} molecules adsorb on a Pt surface at the open circuit potential.

Traditionally, PEG is classified as a throwing power enhancer in metal electrodeposition. However, in the present study we use PEG_{200} not only as an additive, but also as a solvent to dissolve BDA, which is normally dissolved in methanol.

A detailed literature search indicated that few studies have sought to explain the synergetic effect of additives on the deposition of bright Zn coatings. The present study focused on the effect of a mixture of PEG_{200} and BDA on bright Zn deposition. The influence of the additive mixture on the reduction kinetics and morphology was investigated using voltammetry in the stationary diffusion regime, X-ray diffraction (XRD) and scanning electron microscopy (SEM).

2. EXPERIMENTAL PART

The electrochemical study of the reduction of Zn (II) ions in the presence of PEG_{200} and a PEG_{200}/BDA additive mixture was performed in a conventional three-electrode cell using solutions S_0 (= 0.1 M $ZnCl_2$ + 0.32 M H_3BO_3 + 2.8 M KCl, pH = 5.0), S_1 (= S_0 with 1 mM PEG_{200}) and S_2 (= S_0 with 1 mM PEG_{200} + 0.1 mM BDA). The solutions were prepared immediately prior to each experiment using deionized water (18 MΩ cm) and analytical-grade reagents (Aldrich). Before each experiment, the solutions were deoxygenated for 30 min with ultrapure nitrogen (Praxair), and a nitrogen atmosphere was maintained during the experiments. The working electrode was an AISI 1018 steel disc of surface area 0.07 cm^2 enclosed in Teflon, and the steel surface was polished to a mirror finish with 0.05 μm alumina powder (Buehler). The real area of the AISI 1018 steel electrode (A_{real} = 0.101 cm^2) was calculated from additional experiments on the reduction of Zn(II) ions in a base solution (S_0) of composition 0.1 M $ZnCl_2$ + 2.8 M KCl + 0.32 M H_3BO_3, pH = 5.0, using rotating disk electrode (RDE) voltammetry, taking the value of the diffusion coefficient ($D_{Zn(II)}$) to be 8.06 x 10^{-6} cm^2 s^{-1} [19] and using the Levich equation. A saturated calomel electrode (SCE) was used as the reference electrode, and a Pt rod was used as the counter electrode. All potentials reported here are expressed with respect to the SCE. The electrochemical experiments were carried out with an EG &G Princeton Applied Research Potentiostat/Galvanostat (Mod. 273A) coupled to a personal computer equipped with EG&G M270 software for data acquisition.

The adsorption study was performed using a QCM (Maxtek Mod. 710). An AT-cut quartz crystal (f_0 = 5 MHz) covered with an iron film (Maxtek) was used as the working electrode (Fe-QCM) (geometrical area 1.37 cm^2). A new Fe-QCM electrode was used for each experiment. Before each experiment, the electrode was cleaned with degreasing solution. A spectroscopy-grade graphite rod, mounted inside a separate compartment, was used as the counter electrode, and a SCE was used as the reference electrode. To minimize iR-drop effects, a Luggin capillary was employed to connect the reference electrode compartment to the working electrode compartment.

The QCM signal was registered as Δf_{exp} (Hz) (= f-f_0), the experimental frequency change, which can be related to the total mass change at the electrode surface (Δm) using the Sauerbrey equation [41]:

$$\Delta f_{\exp} = -C_f(\Delta m) \quad (1)$$

where C_f ((Hz cm^2) ng^{-1}) is the sensitivity factor of the quartz crystal employed in the measurements. In the present work, C_f was calculated to be 0.056 (Hz cm^2) ng^{-1} using the equation:

$$C_f = \frac{2f_0^2}{\sqrt{\mu_q \rho_q}} \quad (2)$$

where f_0 is the natural frequency of the quartz crystal (f_0 = 5 MHz), μ_q is the shear modulus of the quartz crystal (μ_q = 2.94 x 10^{11} g (cm s^2)$^{-1}$ and ρ_q is the density of the quartz crystal (ρ_q = 2.65 g cm^{-3}).

The surface morphology of the deposits was evaluated using a scanning electron microscope (Jeol, Mod. DSM-5400LV), and the crystal structures were determined by XRD using a Bruker diffractometer (Mod. D8 Advance).

3. RESULTS AND DISCUSSION

3.1. Quartz crystal microbalance (QCM) measurements during additive adsorption at the open circuit potential (E_{OCP}).

Prior to performing the electrochemical study of the reduction of Zn(II) ions in the presence of PEG_{200} or the PEG_{200}/BDA mixture, the adsorption of each additive onto the surface of the Fe substrate at the open circuit potential (E_{OCP} = -0.7 V vs. SCE) was analyzed in independent experiments. Each additive was diluted in a 2.8 M KCl solution and then injected into solution S_0 (0.1 M $ZnCl_2$ + 0.32 M H_3BO_3 + 2.8 M KCl) such that the final concentration of the solution was 1 mM PEG_{200} (solution S_1) or 1 mM PEG_{200} + 0.1 mM BDA (solution S_2).

In each experiment, the additive was added to solution S_0 after the frequency of the microbalance had remained stable ($\Delta f = 0$) for 2 min in solution S_0 alone (with constant agitation). The change in the resonant frequency of the quartz crystal was recorded for 4 min following the addition of the polymer, to monitor the adsorption of the additive (agitation was continued through this 4-min period). Figure 1 shows the changes in mass (calculated using the Sauerbrey equation) observed after PEG_{200} (curve a, Fig. 1) or PEG_{200}/BDA (curve b, Fig. 1) was injected into solution S_0. Immediately after addition of the additive, the mass on the electrode surface increased rapidly and reached a stationary state. After 4 min at the open circuit potential, the change in mass was 3.19 ng cm^{-2} ($\Delta m_{ads}^{PEG_{200},E_{OCP}}$) for the solution containing PEG_{200} and 4.93 ng cm^{-2} for the PEG_{200}/BDA system($\Delta m_{ads}^{PEG_{200}/BDA,E_{OCP}}$) . In a previous study using EQCM and EC-STM, Kim et al. [39] showed that after the initial rapid rise in the mass of polymer adsorbed on the quartz crystal surface, the adsorbed polymer layer enters a stabilization phase in which the adsorbed PEG molecules rearrange into more ordered structures.

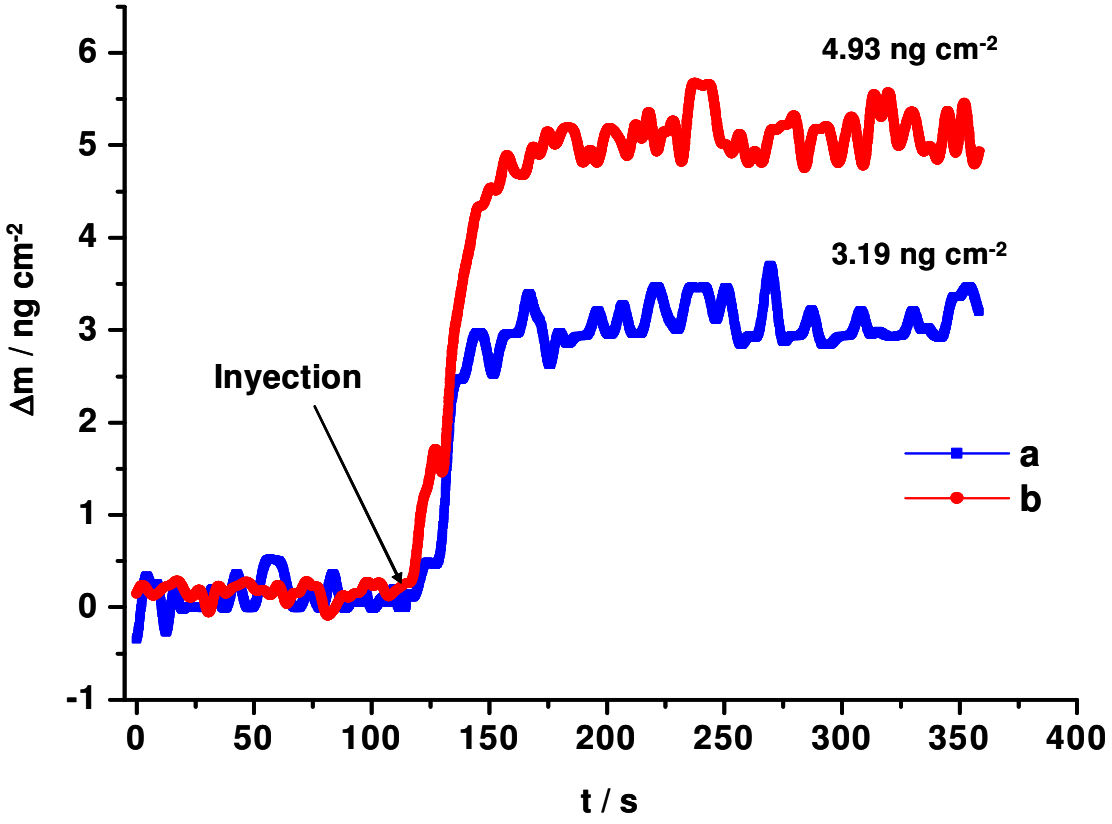

Figure 1. Change in mass (Δm) as a function of time, after addition of the additives to solution S_0 (= 0.1 M $ZnCl_2$ + 0.32 M H_3BO_3 + 2.8 M KCl): (a) 1 mM PEG_{200}, (b) 1 mM PEG_{200} + 0.1 mM BDA.

3.2. Voltammetric study of the electroreduction of Zn(II) ions

The electroreduction of Zn(II) ions on an AISI 1018 steel electrode was studied in solutions S_0, S_1 and S_2 using cyclic voltammetry. The potential scan was initiated in the cathodic direction from the open circuit potential (E_{OCP}).

3.2.1. Without additives

Figure 2 shows a typical voltammogram obtained for solution S_0 (0.1 M $ZnCl_2$ + 0.32 M H_3BO_3 + 2.8 M KCl, pH = 5.0; i.e., without additives). In this system, the reduction proceeds in a single step (peak Ic at -1.12 V vs. SCE) associated with the reduction of Zn(II) ions to Zn(0). On switching the potential scan at -1.55 V vs. SCE and scanning in the positive direction, an anodic peak (Ia) appears, which is associated with the oxidation of Zn(0) formed during the scan in the negative direction.

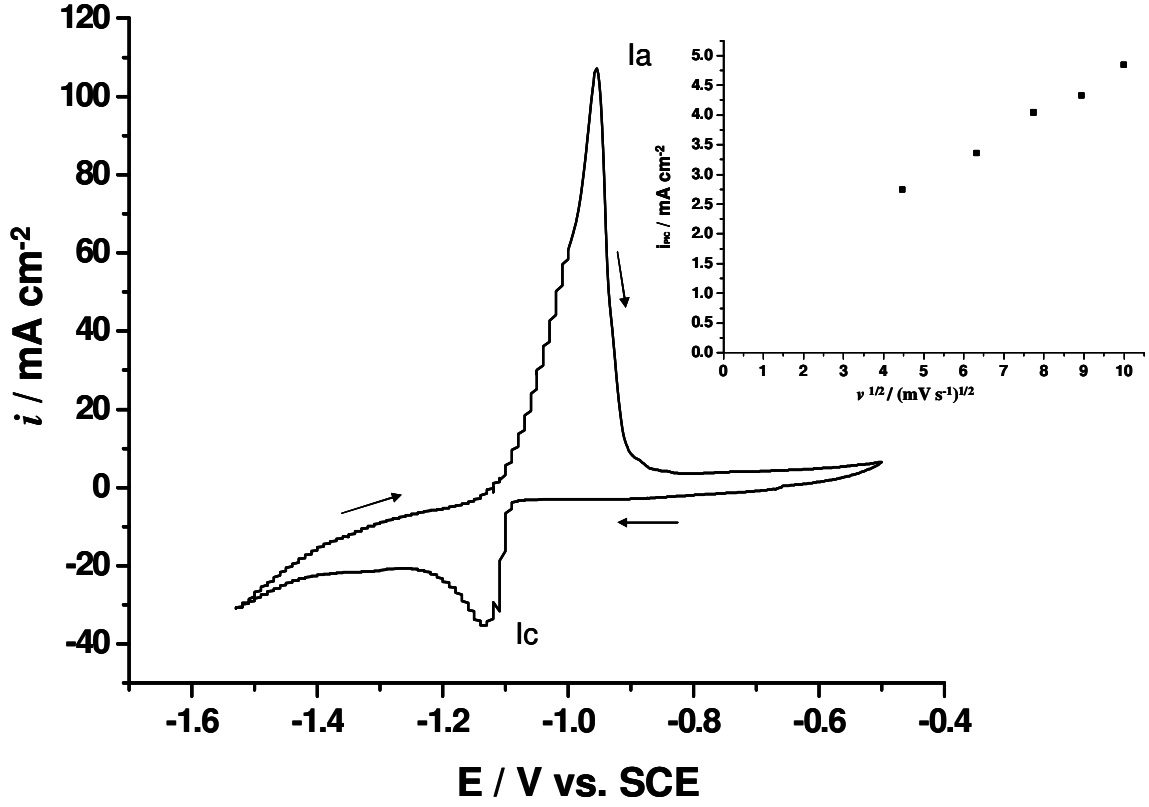

Figure 2. Typical voltammogram obtained using an AISI 1018 steel electrode in a solution of composition S_0, v = 20 mV s^{-1}, T = 25 °C. Inset: variation in the cathodic current density peak with the square root of the scan rate.

In previous studies [19] we have demonstrated that the reduction of Zn(II) ions in solution S_0 involves the species $ZnCl_4^{2-}$, which is reduced to Zn metal via the following reaction:

$$ZnCl_4^{2-} + 2e^- \rightarrow Zn(0) + 4Cl^-$$

The conditional potential associated with this reaction ($E'_{ZnCl_4^{2-}/Zn(0)}$) can be evaluated using Equation 3, which is valid in the pH range from 0.0 to 7.04 [19].

$$E'_{ZnCl_4^{2-}/Zn(0)}(\text{V vs. SCE}) = -1.01 + 0.12\text{pCl}' - 0.03\text{pZn}' \qquad (3)$$

Under the experimental conditions used in this study, $E'_{ZnCl_4^{2-}/Zn(0)}$ has a value of -1.097 V vs. SCE.

Study of the behavior of peak Ic, associated with the reduction of Zn(II) to Zn(0), disclosed that the peak of the current density increased linearly with the square root of the sweep potential rate (i_{pc} vs.

$v^{1/2}$) (Inset of Fig.2). When this graph is extrapolated to $v^{1/2} = 0$, it is found that the intercept is greater than zero. This result indicates that an additional process other than diffusion occurs; this behavior may be attributed to the nucleation phenomena involved, as reported by Hills et al. [42].

3.2.2. In the presence of PEG_{200} and PEG_{200}/BDA.

Immediately after the adsorption of the additives at E_{OCP}, a study of the electrochemical behavior was performed. The influence of PEG_{200} or PEG_{200}/BDA on the electrodeposition of Zn was studied in the potential range -0.5 to -1.55 V vs. SCE using solutions S_1 (= S_0 + 1 mM PEG_{200}) and S_2 (= S_0 + 1 mM PEG_{200} + 0.1 mM BDA).

Figure 3 shows the voltammograms obtained for solutions S_1 (curve *b*, Fig. 3) and S_2 (curve *c*, Fig. 3). For comparison, the voltammogram for the additive-free solution, S_0, is also shown (curve *a*, Fig. 3); the behavior of this system was discussed above in relation to Fig. 2.

The voltammogram obtained in the presence of PEG_{200} (curve b, Fig. 3) resembles that obtained for solution S_0 (curve *a*, Fig. 3). Specifically, the voltammogram exhibits a cathodic peak (I'c) associated with the reduction of Zn(II) ions to Zn(0); the potential at which this peak appears ($E_{PI'C}$ = -1.12 V vs. SCE) is similar to that observed for solution S_0 (curve *a*, Fig. 3) (E_{PIC}=$E_{PI'C}$). In addition, the cathodic current density of peak I'c is less than that of peak Ic. This behavior can be attributed to the adsorption of PEG_{200} molecules on the active sites of the electrode. In addition, the behavior of the voltammogram obtained in the presence of PEG_{200} indicates that the hydrogen evolution reaction is inhibited by the presence of the additive, a finding similar to that reported by Song et al. [25]. Additional experiments (data not shown) showed that the peak of the current density increases linearly with the square root of the sweep potential rate ($i'_{pI'c}$ vs. $v^{1/2}$), indicating that the reduction of Zn(II) ions in the presence of PEG_{200} is diffusion-controlled. When this graph was extrapolated to $v^{1/2} = 0$, it was found that the intercept is greater than zero. This result indicates that an additional process other than diffusion occurs.

During the potential scan in the positive direction, an anodic peak (I'a) is observed at -0.6 V vs. SCE, associated with the oxidation of the Zn(0) deposited during the potential scan in the negative direction.

The presence of PEG_{200}/BDA in the solution (solution S_2, curve c, Fig. 3) induces significant changes in the voltammogram. Two reduction peaks are clearly observed: a small peak, I''c ($E_{PI''c}$ = -1.12 V vs. SCE); and a much larger peak (peak II''c) at more negative potential ($E_{PII''c}$ = -1.22 V vs. SCE). The potential value at which peak I''c ($E_{PI''c}$) appears is the same as that obtained during the reduction of Zn(II) ions in the absence of BDA (peak Ic, curve *a*, Fig.3) (thus, $E_{PIC} = E_{PI'C} = E_{PI''C}$). In addition, the cathodic current density of peak I''c is much less than that of peak Ic. Thus, the formation of peak I''c in the solution containing both PEG_{200} and BDA can be attributed to the electrodeposition of Zn onto the actives sites on the electrode surface that are not blocked by adsorbed PEG_{200} or BDA molecules. At potentials more cathodic than $E_{PI''c}$, the second reduction peak, associated with the bulk deposition of Zn, is observed (peak II''c). The behavior observed during the reduction of Zn(II) ions in solution S_2 (PEG_{200}/BDA) is associated with the adsorption of the additives onto the electrode surface.

The adsorbed additives form an adlayer that almost completely inhibits the discharge of the Zn(II) ions, and blocks most of the active sites at which the first reduction process (peak I''c) occurs. Subsequently, an increase in the overpotential is required for desorption of the additives from the electrode surface, allowing the reduction of Zn(II) ions to take place (peak II''c) at the active sites that are liberated by the desorption of additive molecules. The desorption behavior of the additives PEG and BDA in electrolytic baths has been examined in previous studies. Mockute at al. [38] found that during the reduction of Zn(II) in baths containing BDA, the additive decomposes into diverse compounds. In a study of an electrolytic solution of composition 0.32 M H_3BO_3 + 2.8 M KCl + 1 mM PEG_{20000}, Ballesteros et al. [32] found that the desorption of PEG_{20000} from a Fe electrode occurred in the potential interval -0.6 to -1.6 V vs. SCE.

When the potential scan was switched to the positive direction from -1.55 V vs. SCE, an anodic peak (I''a) was observed, which corresponds to the dissolution of Zn deposited during the scan in the negative direction.

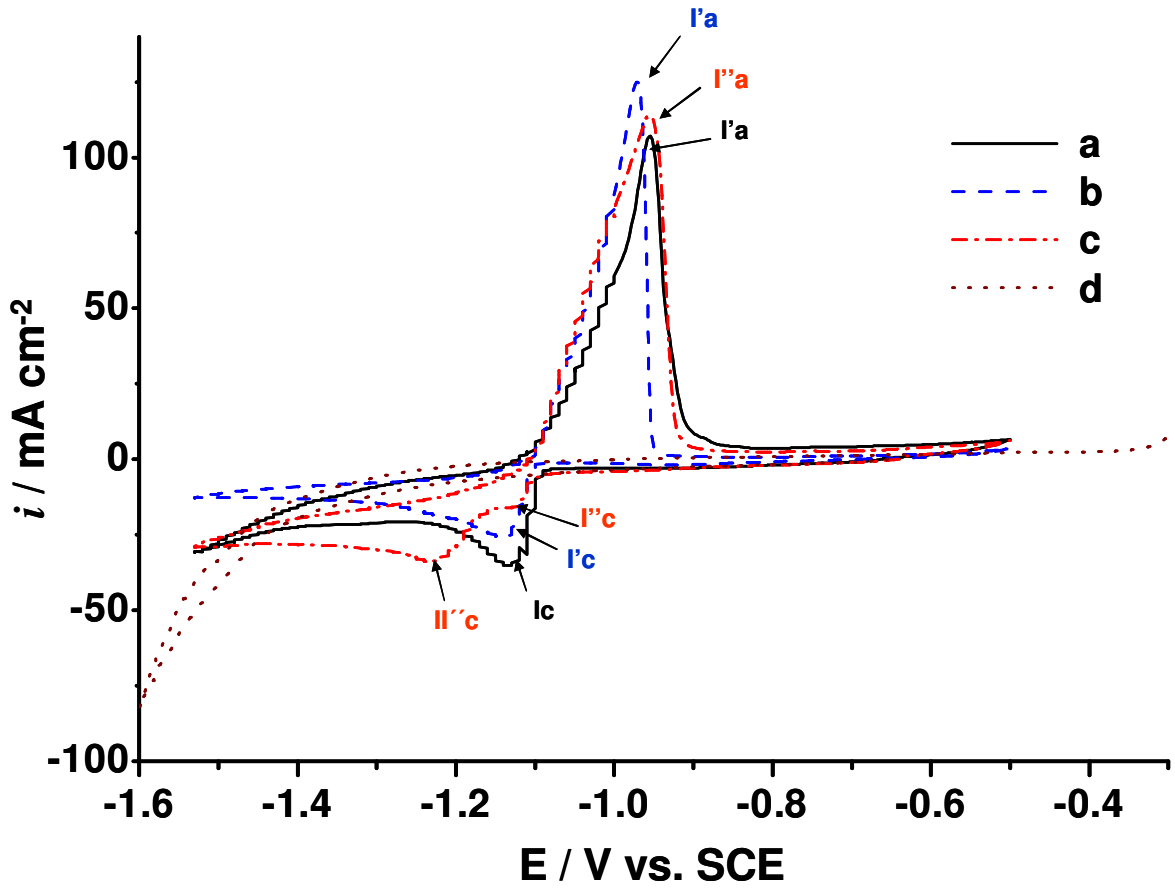

Figure 3. Typical voltammograms for the electroreduction of Zn(II) ions on an AISI 1018 steel electrode, obtained from the following solutions: (a) solution S_0, (b) solution S_1 (= S_0 + 1 mM PEG_{200}), (c) S_2 (= S_0 + 1 mM PEG_{200} + 0.1 mM BDA). (d) The supporting electrolyte 0.32 M H_3BO_3 + 2.8 M KCl + 1 mM PEG_{200} + 0.1 mM BDA is also shown. v = 20 mV s^{-1}.

Table 1 shows the values of the anodic (Q_a) and cathodic (Q_c) charge densities obtained by integrating the voltammograms in Fig.3 over the corresponding potential intervals. When PEG_{200} was added to solution S_0, a lower value of the cathodic charge density and a higher efficiency were obtained. This behavior is associated with the blocking of active sites by additive molecules adsorbed on the electrode surface and with the inhibition of the hydrogen evolution reaction (see curve b, Fig.3).

Among the systems studied, the highest value of the cathodic charge density was obtained when both PEG_{200} and BDA were present in the solution. This behavior can be attributed to the fact that during the reduction process, the cathodic current density has contributions from the current density associated with the reduction of Zn(II) ions and from the decomposition of BDA via a reduction mechanism into diverse compounds, including phenylbutanol, phenylbutanone and phenylbutane [26]. Due to the decomposition of BDA, the cathodic efficiency is lower than that obtained when only PEG_{200} was used as an additive, although it is slightly higher than that obtained in the absence of additives.

Table 1. The total cathodic charge (*Qc*) and total anodic charge (*Qa*), obtained from the voltammograms in Fig. 3.

Solution	*Qc* (mC cm^{-2})	*Qa* (mC cm^{-2})	*Qa Qc*
S_0	616.81	535.04	0.86
S_1	599.97	566.45	0.94
S_2	623.88	559.38	0.89

To analyze the reduction processes associated with peaks I''c and II''c in the voltammogram (curve c, Fig.3), we used the switching potential technique. In these experiments, the switching potential (E_λ) was fixed at the foot of reduction peak I''c or II''c (e.g. $E_\lambda < E_{PI''c}$, $E_{PI''c} > E_\lambda > E_{PII''c}$) and the potential scan was switched to the positive direction at E_λ. The results obtained revealed that the current density of peak I'a depends on both reduction peaks (Fig. 4).

A study of the reduction overpotential ($\eta = E_{PI'c,II'c} - E'_{ZnCl_4^{2-}/Zn(0)}$) ($E_{PI'c,II'c}$, corresponding to the potential of peak I'c or II'c in the presence of additives) for the different solutions was carried out; the results are listed in Table 2. The overpotential associated with peak Ic (η_{rc}) is independent of the presence of additives, whereas the overpotential calculated for peak II''c, observed in the presence of PEG_{200}/BDA, is 100 mV more negative.

These results show that the presence of both PEG_{200} and BDA in the electrolytic bath modifies the mechanism of zinc deposition from a reduction mechanism that involves only one reduction process to a mechanism that involves two reduction processes (peaks I''c and II''c). All of these processes involve the reduction of Zn(II) ions, most likely in the $ZnCl_4^{2-}$ complex form [19]. The overpotential is different for each stage, however, indicating the possible existence of active growth

sites with different energies (I''c and II''c). In this way, the PEG_{200}/BDA mixture not only adsorbs over the electrode surface, but also modifies the mechanism of Zn deposition.

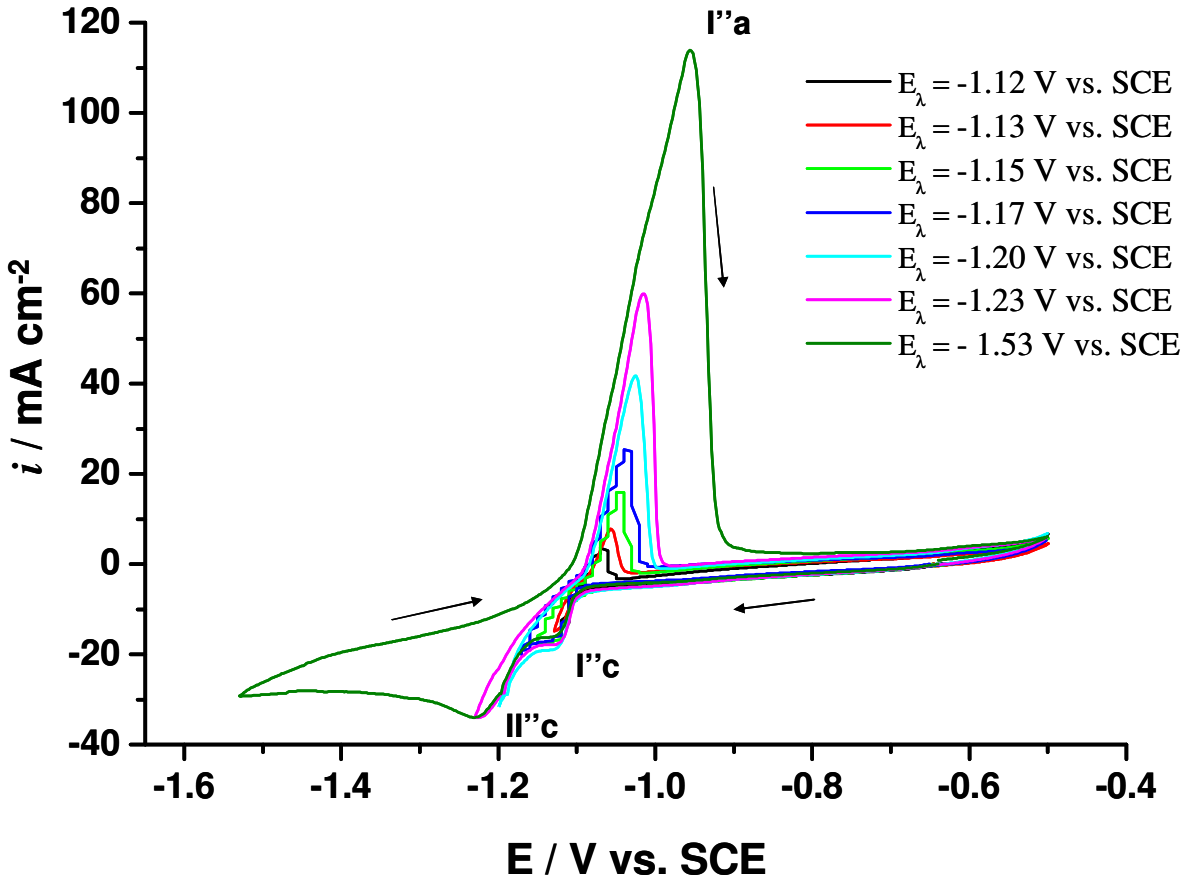

Figure 4. Voltammograms obtained using an AISI 1018 steel electrode in a solution of composition S_2, at different values of the switching potential. v = 20 mV s^{-1}.

Table 2. Overpotential of the reduction of Zn(II) ions on an AISI 1018 steel electrode, obtained from different solutions.

Solution	E_{PIc} (V vs. SCE)	$E_{PII''c}$ (V vs. SCE)	η_1 (E_{PIc} - $E^{\circ}_{ZnCl_4^{2-}/Zn(0)}$)	η_2 ($E_{PII''c}$ - $E^{\circ}_{ZnCl_4^{2-}/Zn(0)}$)
S_0	-1.12	—	-0.023	—
S_1	-1.12	—	-0.023	—
S_2	-1.12	-1.22	-0.023	-0.123

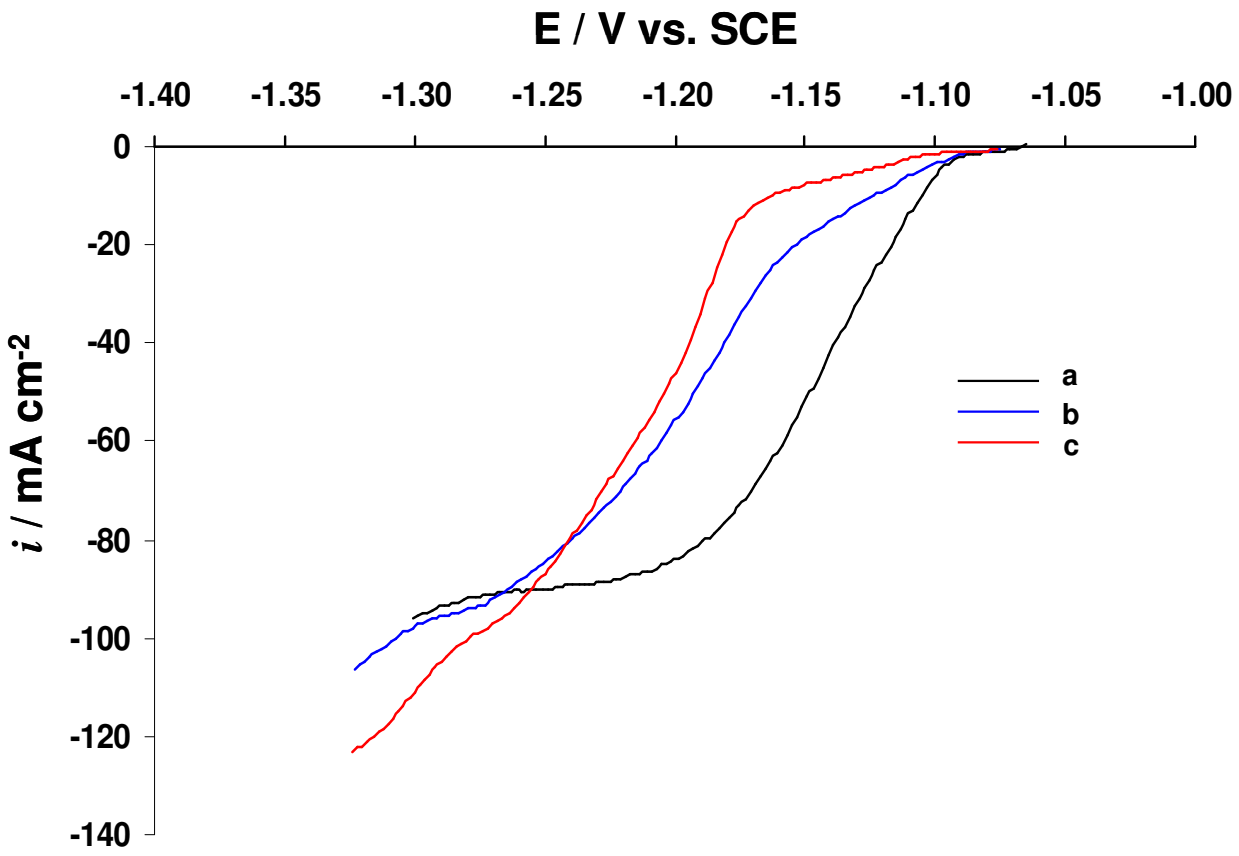

Figure 5. Typical linear voltammograms recorded using an RDE, obtained during the electroreduction of Zn(II) ions in different solutions: (a) solution S_0, (b) solution S_1, (c) solution S_2. ω = 1400 rpm, v = 3 mV s^{-1}.

3.3. Electrodeposition of Zn in the stationary diffusion regime

The electrochemical reduction of Zn in the stationary diffusion regime was studied using the rotating disk electrode (RDE) voltammetry technique. A constant potential scan rate (3 mV s^{-1}) was imposed and the electrode rotation rate (ω) was varied from 1000 to 2000 rpm. Before each run, a Zn predeposit was prepared in situ on the disk AISI 1018 steel electrode by applying 28 mA cm^{-2} for 20 s.

Figure 5 shows the curves of *i vs.* E obtained under these conditions for the reduction of Zn(II) ions from solutions S_0 (no additives, curve *a*), S_1 (with PEG_{200}, curve *b*) and S_2 (with PEG_{200}/BDA, curve *c*). The data show the following characteristics: in the presence of PEG_{200} (curve *b*, Fig. 5) and PEG_{200}/BDA (curve *c*, Fig. 5), the cathodic polarization in the curves increases with respect to that observed in the absence of additives (curve *a*), with the effect being greater in the system with PEG_{200}/BDA. This increase in cathodic polarization is associated with the adsorption of the additives on the electrode surface [36,38], a fact reflected by the progressive decrease of the cathodic current density for potential values greater than -1.25 V vs. SCE. When the potential is close to -1.25 V vs. SCE, the current densities associated with the reduction of Zn(II) ions in the absence and presence of

PEG_{200} are similar, indicating that in this potential region the active sites for the reduction of Zn(II) ions that had been blocked by adsorbed PEG_{200} molecules are now unoccupied. In addition, in the same potential region, the cathodic current density is higher when the PEG_{200}/BDA additive mixture is present in the solution (curve *c*, Fig. 5), suggesting that the presence of both PEG_{200} and BDA in the electrolytic solution leads to an increase in the density of nucleation sites of Zn. This enhanced nucleation rate results in fine-grained zinc deposits.

For each of the three solutions, the limiting current density (i_{lim}) exhibited a linear variation with $\omega^{1/2}$, as can be seen in Figure 6. This behavior demonstrates that, both in the absence and presence of the additives, the reduction of Zn(II) ions is limited by mass transfer of the electroactive species. Extrapolating the curves $i_{lim.}$ *vs.* $\omega^{1/2}$ to $\omega^{1/2} = 0$ yields a nonzero current density for all three systems, indicating that the current density is additionally enhanced by other phenomena coupled to the charger-transfer process.

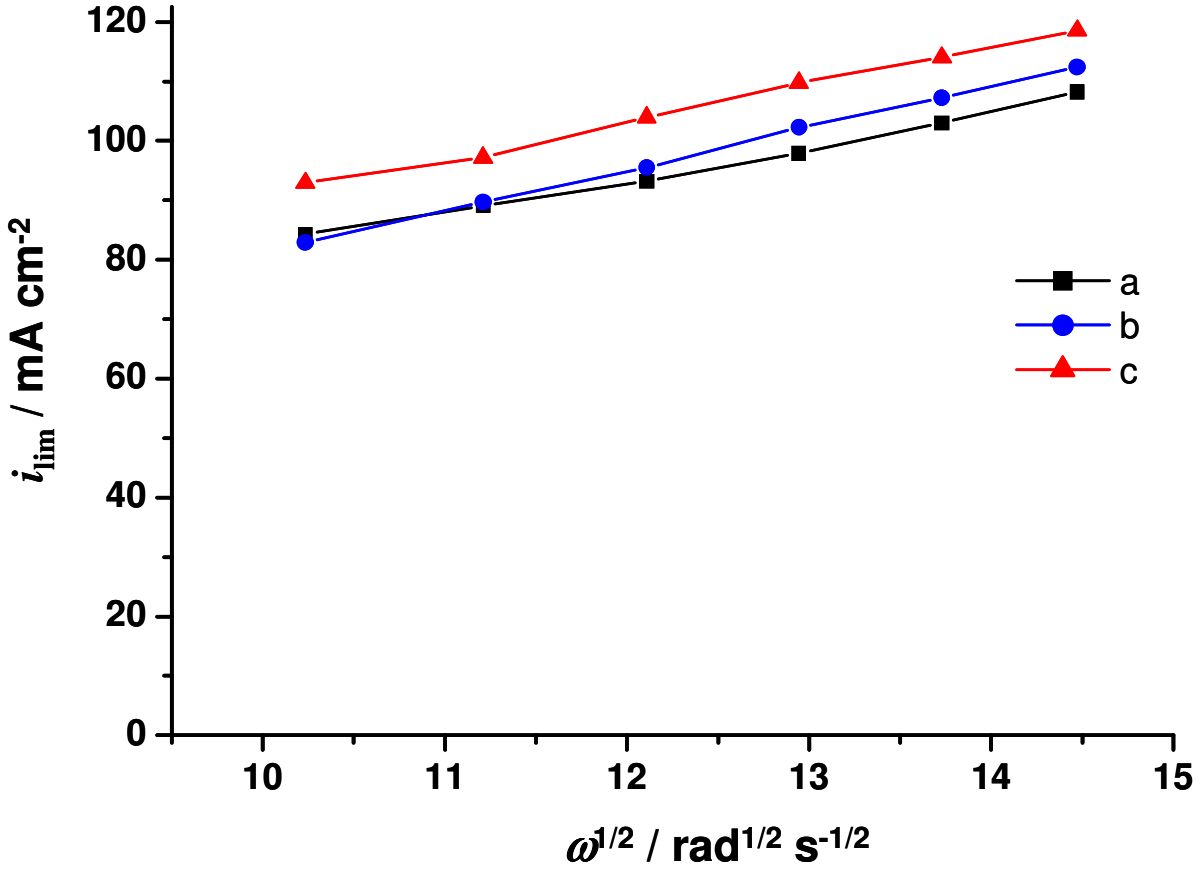

Figure 6. Variation in the cathodic limiting current density with agitation, obtained from different solutions: (a) solution S_0, (b) solution S_1, (c) solution S_2.

To evaluate the kinetic parameters, the current densities free from diffusional effects, i_k, were evaluated by plotting i^{-1} *vs.* $\omega^{-1/2}$ for several constant overpotentials and extrapolating to $\omega^{-1/2} = 0$, according to the equation:

$$\frac{1}{i} = \frac{1}{i_k} + \frac{1.61\nu^{1/6}}{nFD^{2/3}C_0^*\omega^{1/2}} \qquad (4)$$

where F is the Faraday constant, ν is the kinematic viscosity, n is the number of exchanged electrons (n = 2) and C_0 is the Zn(II) concentration.

Figure 7 shows typical i^{-1} *vs.* $\omega^{1/2}$ curves obtained for solutions S_0, S_1 and S_2 at several overpotentials. The values of i_k were obtained from the intercepts.

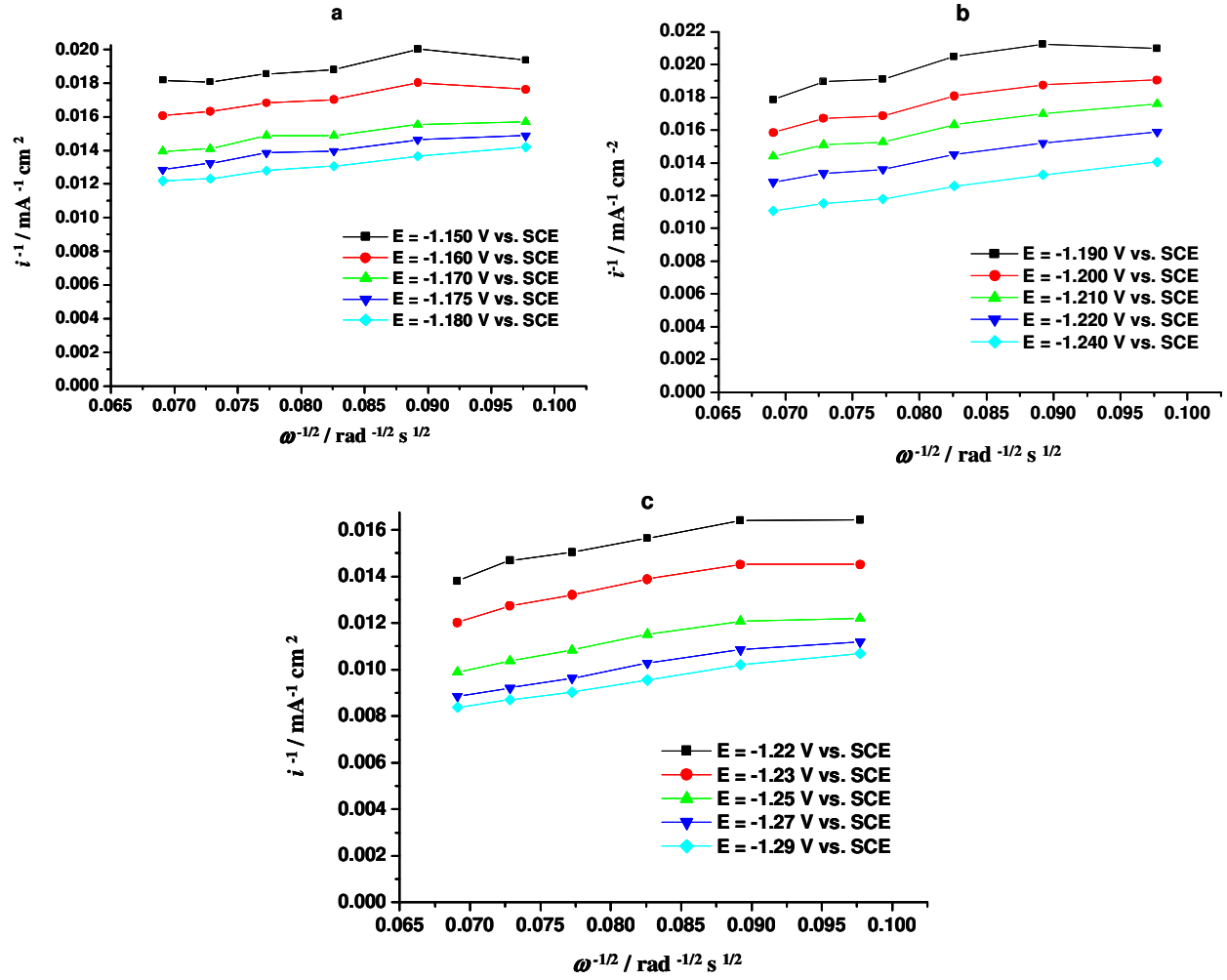

Figure 7. Typical plots of i^{-1} vs. $\omega^{-1/2}$ recorded at various potentials in different solutions: (a) solution S_0, (b) solution S_1, (c) solution S_2.

Using the pure kinetic current density (i_k) for each overpotential, it was possible to estimate the kinetic parameters by means of the rate equation related to a cathodic process under activation control, that is, the Tafel equation:

$$i_k = i_0 \exp\left[\frac{-\alpha_c nF}{RT}\eta\right] \quad (5)$$

where α_c is the charge transfer coefficient, η is the overpotential, and i_0 is the exchange current density.

The Tafel plots obtained for the three solutions are shown in Figure 8. For each system, a well defined linear region is obtained in plots of $\log|i_k|$ against the overpotential η. From the slope and intercept of the plot for each electrolytic solution, it is possible to obtain the values of the cathodic charge transfer coefficient (α_c) and i_0, respectively.

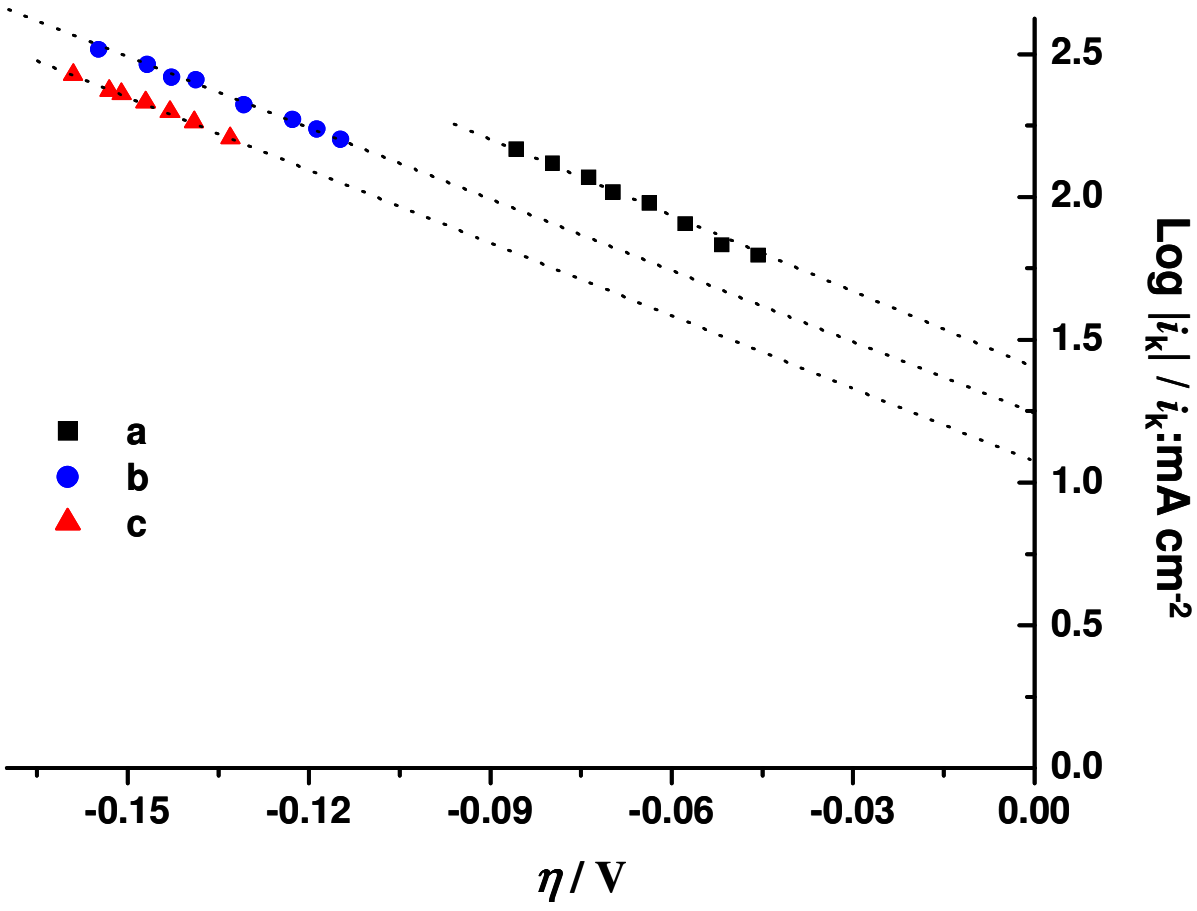

Figure 8. Tafel plot for the reduction of Zn in different solutions: (a) solution S_0, (b) solution S_1, (c) solution S_2.

The calculated values of the electrochemical kinetic parameters α_c and i_0 are listed in Table 3. The value of i_0 decreases from 22.7 to 16.9 mA cm^{-2} when PEG_{200} is added to the solution, and then shows a further decrease to 11.7 mA cm^{-2} when both PEG_{200} and BDA are used as additives. These findings indicate that the reduction kinetics are slower in the presence of the additives, with the solution containing PEG_{200}/BDA showing the lowest rate of Zn(II) reduction. Thus, less crystal growth is expected in solutions containing the PEG_{200}-BDA additive mixture.

In addition, the value of the charge transfer coefficient (α_c) decreases from 0.28 for solution S_0 to 0.24 for solutions S_1 and S_2. This decrease in α_c is associated with differences in the morphological characteristics of the deposits obtained from the different solutions.

Table 3. Kinetic parameters for the electroreduction reaction of Zn obtained from different solutions, determined using the Tafel method.

Solution	Tranfer coefficient (α_c)*	Exchange current density (i_0)* (mA cm^{-2})
S_0	0.28 ± 0.014	22.7 ± 0.33
S_1	0.24 ± 0.015	16.9 ± 0.25
S_2	0.24 ± 0.010	11.7 ± 0.35

* With standard deviation

3.4. Characterization of the Zn coatings

The zinc coatings obtained from solutions S_0, S_1 and S_2 were analyzed using SEM and XRD to determine the influence of the PEG_{200} and PEG_{200}/BDA additives on the morphology and crystallographic orientation of the deposits. The deposits were grown potentiostatically at different potential values, E_{dep} = -1.17 V vs. SCE for S_0, -1.26 V vs. SCE for S_1 and -1.28 V vs. SCE for S_2, until a charge equivalent to a thickness of 10 μm was obtained.

The results show that both the morphology and grain size are affected by the presence of the additives. In the absence of additives (Fig. 9), the Zn coating is comprised of hexagonal plates (Figure 9a) (typical of pure Zn coatings [1,43]) of similar size (~100 μm^2) that grow in multilayers. XRD analysis (Fig. 9b) of this coating showed that the crystals grow predominantly with a (101) crystallographic orientation. These characteristics cause the Zn coatings to have a dark appearance and to be poorly adherent.

In contrast to the morphology of the Zn coatings formed in the absence of additives, the coatings formed in the presence of PEG_{200} are composed of flakes grouped in hemispherical clusters (Fig. 10a) with various sizes (400 to 1900 μm^2). XRD analysis of this coating (Fig. 10b) revealed that the coatings that formed in the presence of PEG_{200} grew in various orientations, principally (101) but with considerable amounts of (002), (100) and (102). Thus, the addition of PEG_{200} to the electrolytic

solution induces significant changes in the morphology and crystallographic orientation of the Zn coatings. The deposits formed in the presence of PEG_{200} were gray in color and exhibited moderate adherence.

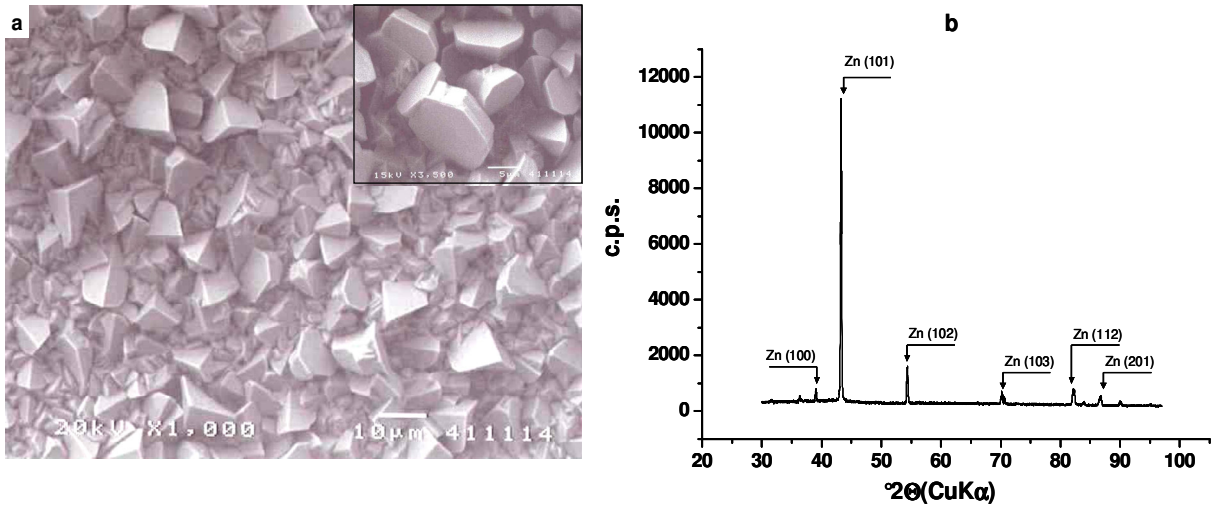

Figure 9. (a) X-ray diffraction (XRD) pattern and (b) a SEM image of a Zn coating electrodeposited at E = -1.17 V vs. SCE, t = 13 min from solution S_0.

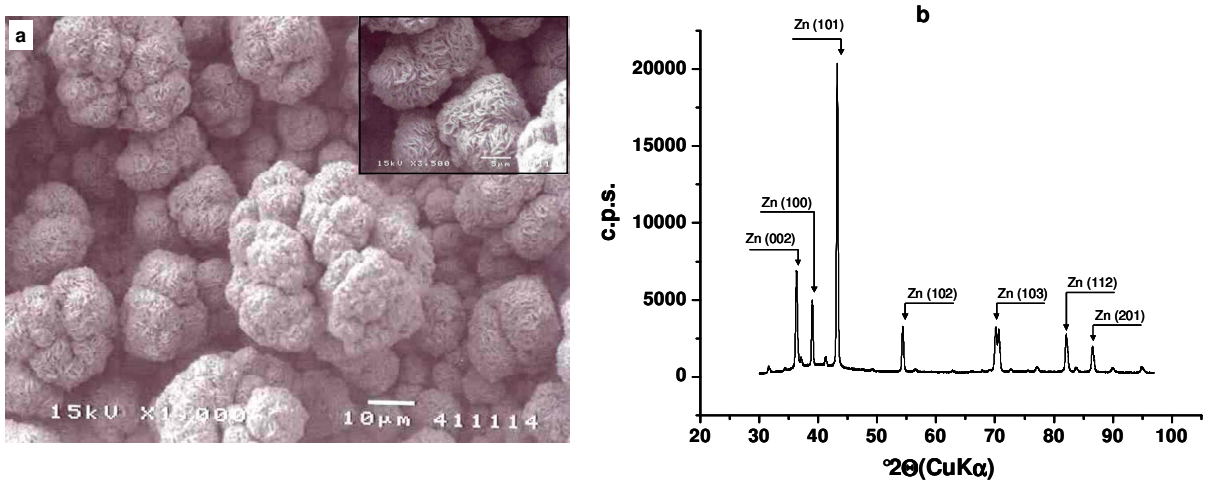

Figure 10. (a) X-ray diffraction (XRD) pattern and (b) an SEM image of a Zn coating electrodeposited at E = -1.26 V vs. SCE, t = 13 min from solution S_1.

The coatings formed in the presence of the PEG_{200}/BDA additive mixture exhibited a morphology and crystallographic orientation similar to those of the coatings obtained in the presence

of PEG_{200} alone. However, a greater number of similarly-sized clusters (~200 μm^2) was observed in the Zn coatings formed in the presence of PEG_{200}/BDA compared to PEG_{200} alone. This finding suggests that in the presence of the additive mixture, the nucleation rate is higher and the crystal growth rate is lower, as predicted on the basis of the calculated values of i_0. This effect can be attributed principally to the adsorption of the additives on the electrode surface. Previously, we have shown that the additives PEG [31] and BDA [44] do not form complexes with Zn(II) ions, indicating that they influence the electrolytic process primarily through their effect on the electrode surface. The coatings that formed in the presence of the PEG_{200}/BDA additive mixture were metallic gray in color, smooth, compact and adherent.

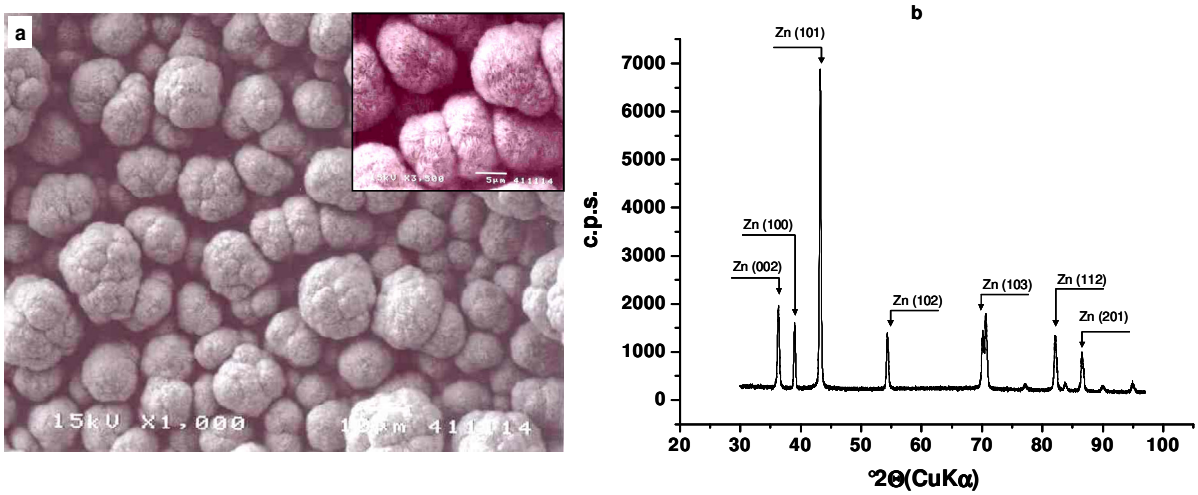

Figure 11. (a) X-ray diffraction (XRD) pattern and (b) an SEM image of a Zn coating electrodeposited at E = -1.28 V vs. SCE, t = 13 min from solution S_2.

4. CONCLUSIONS

In the present study of Zn electrodeposition, the effects of adding PEG_{200} or a mixture of PEG_{200} and BDA to a slightly acidic electrolytic chloride bath were investigated. The following effects were found:

Both PEG_{200} and the PEG_{200}/BDA mixture adsorbed on the Fe surface at the open circuit potential. In addition, the mass adsorbed onto the surface was greater when the solution contained both PEG_{200} and BDA compared to PEG_{200} alone. The adsorption of the PEG_{200}/BDA induced important changes in the electroreduction mechanism of Zn(II) ions, as well as in the morphology and crystallographic structure of the Zn coatings obtained. Specifically, in the absence of additives and in the presence of PEG_{200}, the electroreduction mechanism of Zn(II) ions is similar: a single reduction process, corresponding to massive Zn deposition (bulk deposition), was detected at E_{Pc} = -1.12 V vs. SCE.

Different behavior was observed, however, when both PEG_{200} and BDA were present in the electrolytic bath. In this case two reduction processes were observed: one of low intensity at -1.12 V vs. SCE (peak I''c) and another of greater intensity (peak II''c) at -1.22 V vs. SCE, where the latter feature is associated with the bulk deposition of Zn. The reduction process I''c occurs at the same potential as the single process observed in the systems without additives and with PEG_{200} alone (peaks Ic and I'c respectively). The low intensity of the reduction process I''c is associated with the adsorption of PEG_{200} and BDA molecules on the electrode surface. The adsorbed additive molecules form an adlayer that blocks the active sites required for the first reduction process (peak I''c). Hence, an increase in the overpotential is required for the desorption or decomposition of the additive molecules adsorbed on the electrode surface, allowing the reduction of Zn(II) ions (bulk deposition) to occur (peak II''c) on the liberated active sites.

The adsorption of the additives on the electrode surface additionally induced a decrease in the exchange current density (i_0), resulting in a slowing of the reduction kinetics. In addition, α_c decreased slightly; this decrease can be attributed to the different morphological characteristics of the deposits obtained in the presence of the additives.

Finally, the SEM and XRD studies showed that the presence of the additives in the electrolytic bath induced significant changes in the morphological characteristics of the Zn coatings. In the absence of additives, the Zn coating was comprised of hexagonal clusters (as is typically observed for pure Zn coatings) of similar size (~100 μm^2) with a (101) preferential orientation. When Zn was deposited in the presence of PEG_{200} alone, the resulting coating was comprised of flakes grouped in hemispherical clusters, with sizes ranging from 400 to 1900 μm^2, and exhibited different crystallographic orientations (e.g. (101), (002), (100)). Similar behavior in terms of morphology and crystallographic orientation was observed for coatings grown in the presence of the PEG_{200}/BDA additive mixture. However, an important difference was that in the Zn coating obtained in the presence of the PEG_{200}/BDA mixture, the hemispherical clusters had similar sizes (~200 μm^2). The Zn coating obtained in the presence of the PEG_{200}/BDA mixture was metallic gray in color, smooth, compact and shiny.

The present findings thus indicate that the PEG_{200} additive not only acts as a solvent for BDA but also has an important positive influence on the morphological characteristics of the Zn coating.

ACKNOWLEDGEMENTS

The authors are grateful for financial assistance provided by CONACyT, projects 48440-Y and 48335-Y. L.E. Morón is grateful to CONACyT for scholarship support.

References

1. G. Barceló, M. Sarret, C. Müller and J. Pregonas, *Electrochim. Acta,* 43 (1988) 13
2. S. Rajendran, S. Bharanti, C. Krishna, *Plat. Surf. Finish.,* 84 (October 1997) 53
3. A. Y. Hosny, M.E. El-Rofei, T.A. Ramadan and B.A. El-Gafari, *Metal Finish.,* 93 (November 1995) 55
4. K.L. Lin, C. F. Yang and J.T. Lee, *Corrosion,* 47 (1991) 9
5. B. Bozzini, V. Accardi, P.L. Cavalloti and F. Pavan, *Metal Finish.,* 97 (May 1999) 33
6. R. Ostrow and R.B. Kessler, *Plating,* 57 (1970) 357

7. M. Monev, L. Mirkova, I. Krastev, Hr. Tsvetkova, St. Rashkov, W. Richtering, *J. Appl. Electrochem.,* 28 (1998) 1107
8. A.S. Kumar, C.S. Raja Pandian, J. Ayyapparaju, G.N.K. Armes Bapu, *Bull. Electrochem.,* 17 (2001) 379
9. H. Yan, J. Downes, P.J. Boden, S.J. Harris, *J. Electrochem. Soc.,* 143 (1996) 1577
10. J. Torrent-Burgues and E. Guaus, *J. Appl. Electrochem.,* 37 (2007) 643
11. T. Boiadjieva, M. Monev, A. Tomandl, H. Kronberger, G. Fafilck, *J. Solid State Electrochem.,* 13 (2009) 671
12. K. Jae-Woo, L. Joo-Yul, P. Su-Moon, *Langmuir,* 20 (2004) 459
13. A. D.S. Baik and D. J. Fray, *J. Appl. Electrochem.,* 31 (2001) 1141
14. S.J. Kim, H.T. Kim, S.M. Park, *J. Electrochem. Soc.,* 151 (2004) C850
15. Kh.M.S. Youssef, C.C. Koch, P.S. Fedkiw, *J. Electrochem. Soc.,* 151 (2004) C103
16. E. Michailova, M. Peykova, D. Stoychev, A. Milchev, *J. Electroanal. Chem.,* 366 (1994) 195
17. K. Raeissi, A. Saatchi and M.A. Golozar, *J. Appl. Electrochem.,* 33 (2003) 635
18. J. Yu, L. Wang, L. Su, X. Ai, H. Yang, *J. Electrochem. Soc.,* 150 (2003) C19
19. G. Trejo, R. Ortega Borges, Y. Meas V, E. Chainet, B. Nguyen and P. Ozil, *J. Electrochem. Soc.,* 145 (1998) 4090
20. DDN Singh, M Dey, V. Singh, *Corrosion,* 58 (2002) 971
21. M. Sanchez Cruz, F. Alonso, J. M. Palacios, *J. Appl. Electrochem.,* 23 (1993) 364
22. J. Yu., H. Yang., X. Ai., Y. Chen, *Russian J. Electrochem.,* 38 (2002) 363
23. D.S. Baik and D. J. Fray, *J. Appl. Electrochem.,* 31 (2001) 1141
24. I. Mirkova, G. Maurin, I. Krastev, C. Tsvetkova, *J. Appl. Electrochem.,* 31 (2001) 647
25. K.D. Song, K.B. Kim, S.H. Han, H. Lee, *Electrochem. Solid State Lett.,* 7 (2004) C20
26. D. Mockute, G. Bernotiene, *Chemija,* 2 (1996) 90
27. G. Bernotiene, D. Mockute, *Russian J. Electrochem.,* 30 (1994) 146
28. I. Kirilova, I. Ivanov, S. Rashkov, *Bulg. Chem. Comm.,* 29 (2) (1996) 355
29. E.M. de Olvera and I.A. Carlos, *J. Appl. Electrochem.* 38 (2008) 1203-1210
30. A. Gomes and M.I. da Silva Pereira, *Electrochim. Acta,* 51 (2006) 1342
31. G. Trejo, H. Ruiz, R. Ortega-Borges, Y. Meas, *J. Appl. Electrochem.,* 31 (2001) 685
32. J.C. Ballesteros, P. Díaz-Arista, Y. Meas, R. Ortega, G. Trejo, *Electrochim. Acta,* 52 (2007) 3686
33. G. Trejo, R. Ortega, Y. Meas, E. Chainet, P. Ozil, *J. Appl. Electrochem.,* 33 (2003) 373
34. L. Joo-Yul, K. Jae-Woo, L. Min-Kyu, S. Hyun.Joon, K. Hyun-Tae, P. Su-Moon, *J. Electrochem. Soc.,* 151 (2004) C25
35. K. Jae-Woo, L. Joo-Yul, P. Su-Moon, *Langmuir,* 20 (2004) 459
36. V. Danciu, V. Cosoveanu, E. Grunwald, G. Oprea, *Galvanotechnik,* 94 (2003) 566
37. C. Juhos, S. Mathe, E. Gruenwald, C. Varhelyi, G. Sfintu, *Galvnotechnik* , 83 (1992) 2282
38. D. Mockute, G. Bernotiene, *J. Appl. Electrochem.,* 27 (1997) 691
39. J.W. Kim, J.Y. Lee, S.M. Park, *Langmuir*,20 (2004) 459
40. A. Méndez, P. Díaz-Arista, L. Salgado, Y. Meas, G. Trejo, *Int. J. Electrochem. Sci.,* 3 (2008) 918
41. G. Sauerbrey, *Z, Phys.,* 155 (1959) 206
42. G.J. Hills. D.J. Schiffrin. J. Thompson, *Electrochim. Acta,* 19 (1974) 657
43. H. Yan, J. Downes, P.J. Boden, S.J. Harris, *J. Electrochem. Soc.,* 143 (1996) 1577
44. P. Diaz-Arista, Y. Meas, R. Ortega, G. Trejo, *J. Appl. Electrochem.,* 35 (2007) 217